COBEM 2021 26th International Congress of Mechanical Engineering
November 22-26, 2021, Virtual Congress, Brazil

COB-2021-1138
EVALUATION OF THE WSGG MODEL FOR COUPLED CALCULATIONS OF LAMINAR FLAMES

Pedro Wink Guaragna
Guilherme Crivelli Fraga
Fernando Marcelo Pereira
Francis Henrique Ramos França
Department of Mechanical Engineering, Federal University of Rio Grande do Sul, 425 Sarmento Leite St., Porto Alegre, Brazil
pedro.guaragna@ufrgs.br
guilhermecfraga@gmail.com
Fernando.pereira@ufrgs.br
frfrança@mecanica.ufrgs.br

Abstract. *Combustion gases emit and absorb radiation in a wide range of temperatures however, they do not so continuously regarding the wavelength. Different approaches were developed over the years to replicate this phenomenon, the most widely spread one perhaps being the weighted-sum-of-gray-gases (WSGG), that models the absorption behavior of the real gas as combination of a small number of gray gases. Most works in literature assess the WSGG model by evaluating the radiative heat transfer equation decoupled from the combustion and fluid flow processes, i.e. where the radiation field is computed from predetermined fields of pressure, temperature and species concentration. In practical applications, though, radiation is coupled to all other physical processes, and it is known that inaccuracies in the prediction of the radiation field can lead to errors in other scalars, such as the temperature and the rate of species formation. Therefore, this study carries out an evaluation of different formulations of the WSGG model for coupled radiation-combustion calculations of a set of one-dimensional, laminar flames. The calculations are performed in the CHEM1D code, on which the WSGG model (and the line-by-line integration method, which serves as the benchmark for the comparisons) has been implemented.*

Keywords: *Thermal radiation, combustion gases, WSGG, strain rate*

1. INTRODUCTION

The radiative heat transfer process in participating media is a subject of great importance, especially for the energy generation industry, as in combustion processes thermal radiation is generally the main heat transfer mode, but its reliable computation still is challenging. The radiative properties of absorbing-emitting species have a complex behavior as these are not regularly distributed regarding the wavelength, but rather in specified intervals, called bands, inside which they strongly oscillate. Moreover, radiation in participating media is a volumetric phenomenon, instead of a surface phenomenon, so changes in the temperature and species concentration of the gases throughout space must also be accounted for. Compromise between accuracy and computational costs must be accounted for when modelling the gas radiation in the combustion process.

The weighted-sum-of-gray-gases (WSGG) model approximates the behavior of a gas by representing its spectrum with a few gray gases that occupy certain noncontiguous portions of the spectrum plus a transparent window. The absorption and emission-weighting coefficient associated to each gray gas must be determined, with different works in literature developing iterations of this model with fitting data, usually total emittances, based upon different scenarios. One of the most widely referred work is by Smith et al., 1982, where coefficients were fitted against emittance data computed from exponential wide-band model for typical combustion products of methane and fuel oil. For these fuels, the corresponding partial pressure ratios between water vapor and carbon dioxide are 2/1 and 1/1, respectively.

Other authors also developed correlations for the WSGG model, including Krishnamoorthy, 2010, who based his model for a methane and air, turbulent jet flame with partial pressure ratios varying between 1.5/1 to 4/1, while maintaining maximum error below 10% when compared to spectral line-based WSGG (SLW) benchmark solutions. Dorigon et al., 2013, proposed new coefficients for partial pressure ratios of 2/1 and 1/1 based on the up-to-date HITEMP2010 spectral database and validated the results with line-by-line (LBL) integration of the whole spectrum in several cases of non-isothermal, non-homogeneous problems and results achieved were below 5% in maximum error.

In most cases, the validation and development of the WSGG correlations were made in decoupled calculations of the radiative transfer equation, where temperature and molar concentration data were predefined, either from experimental data or from empirical distribution. In real combustion applications, however, radiation is coupled to all other physical processes, and it thus affects scalars such as the temperature and the reaction rates and formation of species, as well as

the propagation speed and extinction characteristics. On the other hand, changes in the afore mentioned scalars influence the radiative properties of the medium and, as consequence, on the resulting radiation field.

Due to computational costs, spatially demanding simulations of flames are a challenge, the more so if coupled with the RTE. The CHEM1D software developed by Somers, 1994, which solves one dimensional flame structures known as flamelets, proves a powerful tool for solving detailed chemistry flames coupled with the radiative problem. These flamelets represent the transport, chemical kinetics and radiative heat transfer decoupled from flow equations. Therefore, the purpose of the present study is to evaluate different propositions of the WSGG model and compare them with the LBL method regarding the results calculated for the fields of temperature and species concentration, as well as the radiation field. Cases simulated are focused mainly on methane and air combustion, with or without dilution of CO_2 or N_2 in the fuel. Besides these methods, comparisons with calculations that neglect radiation or use the optically thin approximation to account for the radiative transfer are also performed. This work focused its research on counterflow flames, as represented in Figure (1):

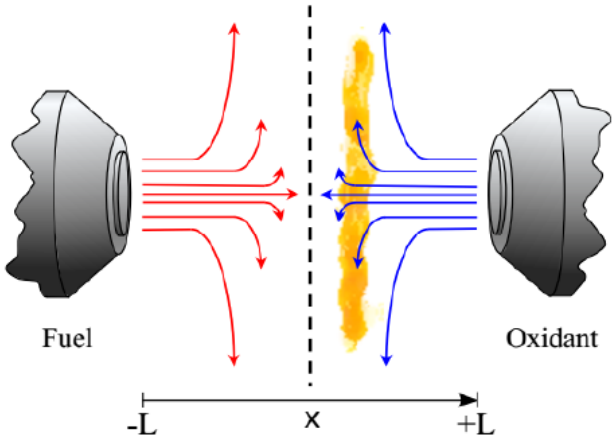

Figure 1: Counterflow flame.

2. RADIATIVE TRANSFER EQUATION AND SPECTRAL MODELLING

Determination of the radiation field in participating media requires the solution of the radiative transfer equation (RTE). For a medium that absorbs and emits radiation, but where scattering is neglected, the RTE is given as (Howell et al., 2016):

$$\frac{dI_\eta(S)}{dS} = -\kappa_\eta(S)I_\eta(S) + \kappa_\eta(S)I_{b\eta}(S) \tag{1}$$

where $I_\eta(S)$ and $I_{b\eta}(S)$ are, respectively, the spectral intensity and the blackbody spectral intensity at position S along a given path. The term κ_η stands as the spectral absorption coefficient. It should be noted that η stands for wavenumber. Considering a gas with uniform conditions of temperature and composition, for example, a well-mixed furnace, then κ_η and $I_{b\eta}$ are constant throughout the volume and integration of Eq. (1) from *0* to *S* will yield:

$$I_\eta(S) = I_\eta(0)e^{-\kappa_\eta S} + I_{b\eta}[1 - e^{-\kappa_\eta S}] \tag{2}$$

where $e^{-\kappa_\eta S}$ stands for the spectral transmittance. The integration of the RTE over all the spectrum will result in the total absorptance along the uniform path:

$$\alpha(S) = \frac{\int_0^\infty I_\eta(0)\alpha(S)d\eta}{\int_0^\infty I_\eta(0)d\eta} = \frac{\int_0^\infty I_\eta(0)\left[1-e^{-\kappa_\eta S}\right]d\eta}{\int_0^\infty I_\eta(0)d\eta} \tag{3}$$

It is more convenient, in order to evaluate the absorptance of the gas, to consider the integral of Eq. (3) in terms of a single broadened line η_{ij} where, therefore, the absorption coefficient κ_{ij} is essentially null except in a narrow wavenumber range surrounding this single line. The intensities $I_\eta(0)$ and $I_{b\eta}$ remain essentially constant within this range. The integration becomes:

$$\alpha_{ij}(S) = \frac{I_{\eta_{ij}}(0)\int_{-\infty}^{\infty}\{1-exp[-\kappa_{\eta,ij}S]\}d(\eta-\eta_{ij})\eta}{\int_0^{\infty} I_\eta(0)d\eta} \tag{4}$$

Also of importance in the validation of models for participating media, is the definition of the total emittance. This solution is for an absorbing gas "*a*" that is mixed with other gases "*r*", non-participating, in an isothermal (with value of *T*), homogeneous media along the path *S*:

$$\varepsilon_a(T,p_a\cdot S) = \frac{\int_{\eta=0}^{\infty} I_{\eta b}(\eta,T)\cdot 1 - e^{(-\kappa p\eta,a\cdot p_a\cdot S)}d\eta}{\sigma T^4/\pi} \tag{5}$$

where $I_{\eta b}$ is the spectral intensity of radiation of the black body (given by the Planck distribution):

$$I_{\eta b}(\eta,T) = \frac{2C_1\eta^3}{exp(C_2\eta/T)-1} \tag{6}$$

in which C_1 is the first Planck's constant, equal to 0.59552137×10^{-12} Wcm^2/sr.

2.1 The weighted-sum-of-gray-gases (WSGG) model

The WSGG model represents the spectrum in its entirety with only a few gray gases with a uniform pressure absorption coefficient, plus a transparent window. The model assumes that the *i*th gas covers a fixed, noncontiguous portion of the spectrum, $\Delta\eta_i$ and that the pressure absorption coefficient $\kappa_{p,i}$ is independent of the temperature *T* and of the partial pressure p_a of the participating species. Both considerations serve as a stricter form of scaling approximation, as in this way, the dependence the absorption coefficient has on the wavenumber and on the thermodynamic state (temperature and molar concentrations) are decoupled.

Integrating Eq. (5) over the spectrum with the WSGG model, the total emittance becomes:

$$\varepsilon(T,p_a\cdot S) = \sum_{i=1}^{I} a_i(T)\left[1 - exp\left(-\kappa_{p,i}p_a S\right)\right] \tag{7}$$

in which $a_i(T)$ is the fraction of the blackbody emission in the range of the spectrum corresponding to the *i*th gray gas, as determined from the fitting. The parameters from WSGG that are calculated from the fitting expression can be used to solve general radiation problems, not being limited only to isothermal, uniform medium. This fitting to emittance data with Equation (7) allows obtaining the pressure absorption coefficients $\kappa_{p,i}$ of each gray gas as well as the temperature dependent coefficients $a_i(T)$ which can be represented by polynomial functions:

$$a_i(T) = \sum_{j=1}^{J} b_{i,j}T^j \tag{8}$$

In the above equation, $b_{i,j}$ is the polynomial coefficient of *j*th order for the *i*th gray gas. The temperature dependent coefficients are calculated as above only for the gray gases, in order for the radiation energy to remain conserved, and so the transparent window is calculated as:

$$a_o(T) = 1 - \sum_{i=1}^{I} a_i(T) \tag{9}$$

The determination of these coefficients varies from author to author with each using the fitting data that best responded to their benchmark comparisons. As part of the simplification proposed by the WSGG, the total radiation intensity in a certain direction is computed by the summation of the intensities I_i related to each gray gas:

$$I(S) = \sum_{i=1}^{I} I_i(S) \tag{10}$$

where this partial intensity I_i can be obtained through integration, as mentioned above, of Equation (1) applied to a single gray gas:

$$\frac{dI_i(S)}{dS} = -\kappa_{p,i}p_a(S)I_i(S) + \kappa_{p,i}p_a(S)a_i(S)I_b(S) \tag{11}$$

in which $p_a(S)$ is the partial pressure of the participating species, $a_i(S)$ is the temperature dependent coefficient and $I_b(S)$ is the total intensity of the blackbody evaluated at local conditions (at position *S*). Therefore, although the WSGG model assumes that the pressure absorption coefficient is constant, the temperature dependent coefficient and the partial pressure terms can account for changes in temperature and molar concentrations, allowing the application of the model in non-isothermal, non-homogeneous media.

2.2 The line-by-line integration

The LBL integration method stands as the benchmark solution of the spectral dependency for the radiative problem, as it can be considered exact except for minor numerical approximations in the integration of the lines. The method is based on the discretization in terms of the wavenumber of the spectral properties available in the extensive database HITEMP2010 provided by Rothman *et al.*, 2010. This present study employed a code provided by the LRT-UFRGS laboratory that ranged from 0 to 10000 cm^{-1} with a spectral resolution of 150000. Detailed information on the generation of the absorption spectra used for the LBL calculations carried out in this paper can be found in Fraga et al., 2019, 2020.

2.3 The Discrete Ordinates Method (DOM)

In order to integrate the spatial domain, the discrete ordinates method was applied, although it should be noted that the WSGG can be solved with any other method of solving the spatial domain. In the conditions of this work, where the participating media is bounded by two parallel surfaces that have black body properties and set at the constant temperature of 298 K. The method solves the spectral intensity in a forward, $I_{i,l}^{+}(s)$, and a backward $I_{i,l}^{-}(s)$, direction, as depicted in Figure (2) with the resulting RTE having the form:

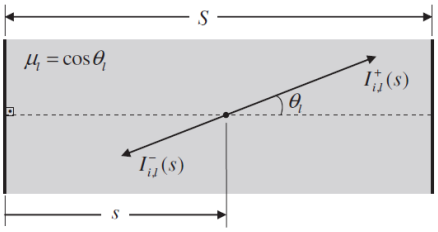

Figure 2. Schematic of the one-dimensional domain. Adapted from Dorigon et al., 2013

$$\mu_l \frac{dI_{i,l}^{+}(s)}{ds} = -\kappa_{p,i} p_a(s) I_{i,l}^{+}(s) + \kappa_{p,i} p_a(s) a_i(s) I_b(s) \tag{12a}$$

$$-\mu_l \frac{dI_{i,l}^{-}(s)}{ds} = -\kappa_{p,i} p_a(s) I_{i,l}^{-}(s) + \kappa_{p,i} p_a(s) a_i(s) I_b(s) \tag{12b}$$

where μ_l represents the cosine in the *l* direction. After solving Eqs. (12a) and (12b), one can calculate the net radiative heat flux and volumetric source in position s, respectively through the equations:

$$q_R''(s) = \sum_{i=0}^{I} \sum_{l=1}^{L} 2\pi \mu_l w_l \left[I_{i,l}^{+}(s) - I_{i,l}^{-}(s) \right] \tag{13a}$$

$$\dot{q}_R(s) = \sum_{i=0}^{I} \sum_{l=1}^{L} 2\pi w_l \kappa_{p,i} p_a(s) \left\{ \left[I_{i,l}^{+}(s) + I_{i,l}^{-}(s) \right] - 2 a_i(s) I_b(s) \right\} \tag{13b}$$

In which w_l is the quadrature weight for l direction. An important direct consequence of the Equations (12) and (13) is that the WSGG model is intrinsically conservative since the radiative energy balance is satisfied as $\dot{q}_R(s) = -dq_R''(s)/ds$. This factor is crucial when radiation is coupled with other heat transfer mechanisms in the global energy equation.

3. NUMERICAL METHOD AND WORK METHODOLOGY

The CHEM1D software solves the transport equations for the conservation of mass, conservation of chemical species and conservation of energy according to the flamelet formulation proposed by de Goey *et al.*, 1999, with assumptions of laminar flame and low Mach number. Since the calculations are for one-dimensional analysis, a stretch rate K is introduced to account for the effects of multidimensionally not present in the 1D scenario, whose conservation equation is written as:

$$\frac{\partial(\rho u K)}{\partial x} = \frac{\partial}{\partial x}\left(\mu \frac{\partial K}{\partial x}\right) - \rho K^2 + (\rho a^2)_{ox} \tag{14}$$

in which ρ is the specific mass, u is the velocity in the x direction, μ is the dynamic viscosity of the mixture and the term a here stands for the strain rate at the oxidant side, and is written as:

$$a = -\frac{\partial u}{\partial x} \tag{15}$$

this represents the velocity gradient of the flow. When solving the radiative transfer equation, the software brings as input for it the temperature and molar fractions of water vapor and carbon dioxide, as well the position of each volume in the discretization scheme. As an output from the RTE, the result for the radiative volumetric source is added to energy balance equation.

The detailed mechanism DRM19 proposed by Kazakov et al., 1995, which consists of 19 species was used for the chemical kinetics. As noted by Goswami, 2014, this mechanism can show up to 11% in deviations of burning velocity if compared to more detailed mechanism like GRI Mech 3.0 (which consists of 53 species). However, more species inevitable results in higher calculation costs.

Therefore, the simulation settings were of a counterflow flame, with stationary solution, detailed chemistry model, constant Lewis diffusion model.

3.1 Mesh convergence

To ensure that results were not affected by computational errors due to the discretization of the problem, a study regarding the quality of mesh was performed. Four different meshes were applied to the same case, a counterflow methane-air combustion without radiative losses. The meshes M1, M2, M3 and M4 had, respectively, 100, 200, 400 and 800 volumes each. Values evaluated to determine mesh quality were the maximum values of temperature and velocity. Other results, such as species formation for water vapor and carbon dioxide were also included in this analysis but there was no noticeable difference in their formations.

Also, as radiative source term and flux are strongly dependent of temperature and species concentration, this study in mesh independence was made for an adiabatic case. Figure 4.a represents the distribution of volumes in the domain for the three meshes with the temperature profile, while Figure 4.b shows the differences in maximum temperature and velocity. Although there is still a small variation in maximum velocity (less than 2% between M2 and M3, and practically null between M3 and M4), the result for temperature is practically unchanged from M2 to M3 as well from M3 to M4, and for the purpose of this work, this stands as enough validation for a good result in mesh independence. In the following results, all calculations were performed for 400 volumes as results are in an asymptotic range with this mesh.

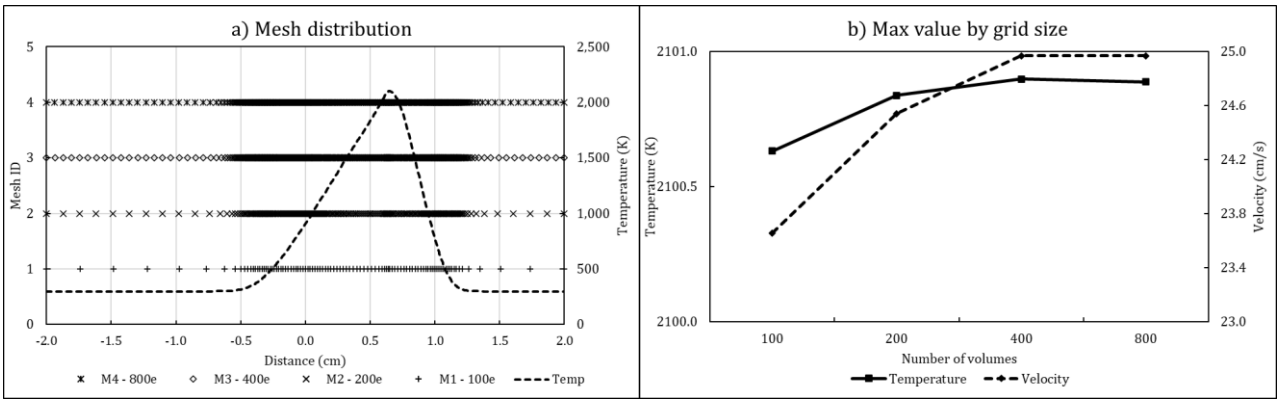

Figure 4. (a) distribution of finite volumes for each mesh; (b) maximum values for temperature and velocity for each mesh

3.2 Comparison with decoupled in-house RTE code

The CHEM1D software already comes with an optical thin approximation (OTA) method for solving the radiative transfer equation, but, since the purpose of this work is to implement in-house codes for the WSGG model and the LBL integratin step, an intermediate step before generating results was to verify if the implementation was according to expected. The LBL and five different variations of the WSGG model were added to the software and comparisons were made between the RTE calculation within the CHEM1D routine and the RTE solved by the in-house code. Figure (3) shows the results for the WSGG implementation with coefficients proposed by Dorigon et al., 2013, and the solution by way of the in-house code for a same input, that is, the same temperature and molar fractions of the species as it was in the convergence of the CHEM1D calculation. Some small difference is noted between both results. This was supposed to be due to approximation error and significant digits calculation. The same procedure was performed for the five implementations of WSGG. Table (1) presents the values of relative error for radiative heat flux and volumetric source for a strain rate of 10 s^{-1}.

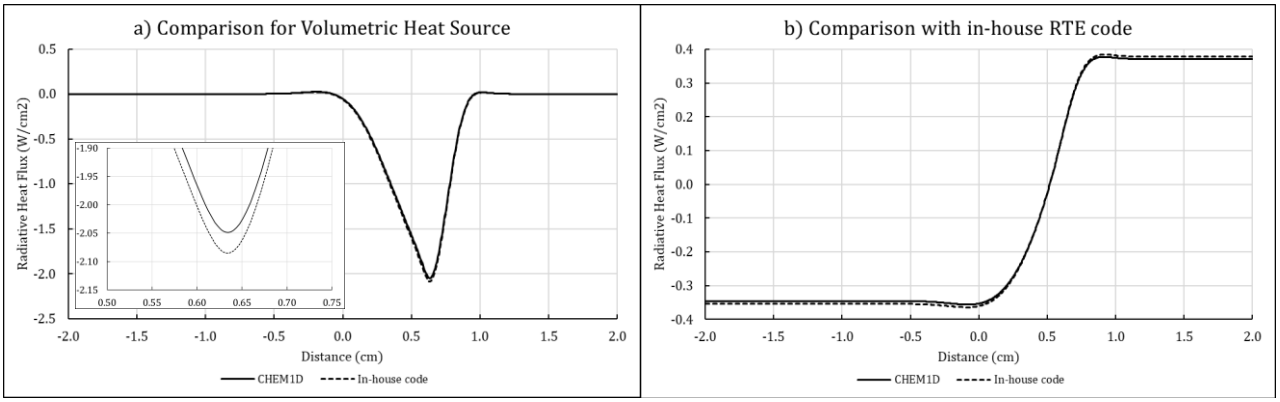

Figure 3. Comparisons between the CHEM1D and in-house code for RTE for (a) radiative volumetric heat source (b) net radiative heat flux

Table 1. Comparisons for Radiative Heat Flux and Volumetric Heat Source between CHEM1D and in-house code. Four different WSGG implementations and the LBL method. Maximum relative error.

Model	q_R''	$\dot{q}_R$
Dorigon 2013	2.7%	1.8%
Krishnamoorthy 2010	3.0%	1.9%
Coelho 2019	2.7%	1.7%
Smith 1982	2.6%	1.8%
Yin 2013	2.2%	1.4%
LBL	2.2%	1.1%

4. RESULTS AND DISCUSSION

Below are the results for the simulated cases. Altogether, for each radiation model applied, cases were calculated for a varying of strain rate values, with them being 5, 10, 20, 50 and 100 s^{-1}. In the first section, results are presented for calculations with the line-by-line solution only.

4.1 Benchmark results for different strain rates

Figure 4a shows the results for the line-by-line method for molar fraction of participating species while Figure 4b shows the comparison for temperature; the different curves are for the strain rates used in the present study. Some interesting result can be perceived. Firstly, the formation of carbon dioxide is more affected by the change in the velocity gradient. There is a 17.0% decrease in the peak value of molar fraction of CO_2 between the case with strain rate of 5 s^{-1} and the one with 100 s^{-1} while for H_2O is of only 3.4%. This can cause a great effect in the applicability of WSGG models and comparison with the benchmark result since many of the implementations were curve-fitted with data with specified molar ratio, such as ratio 2:1 or 1:1.

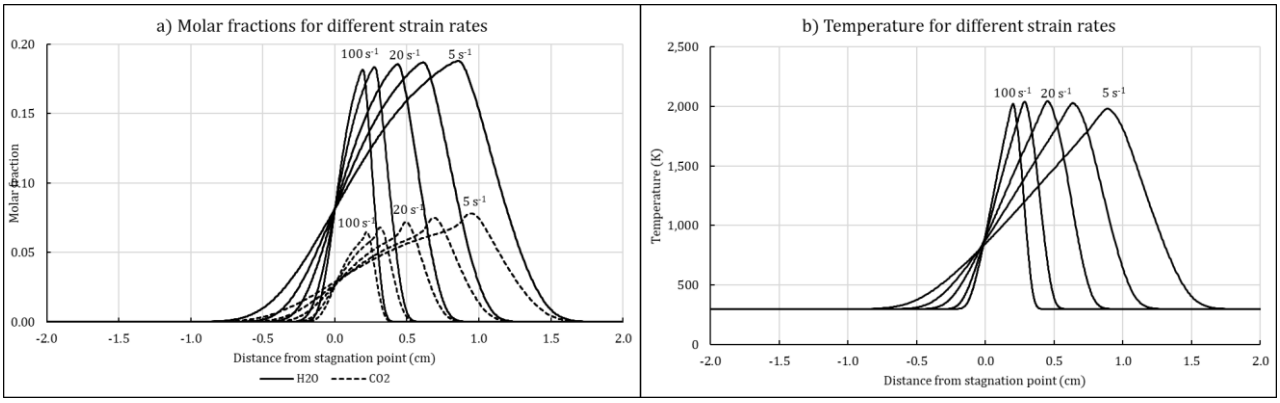

Figure 4. (a) molar fraction over distance and for different strain rates; (b) temperature over distance and for different strain rates.

Secondly, the variation of temperature over different strain rates is not linear. Between the cases simulated, the temperature reached a peak value of 2043K for the strain rate of 20 s^{-1}. To better present the results, Table 2 presents values of molar fraction and temperature. A decrease in the maximum temperature is expected in the lower values of strain rate as the effect of radiative losses become more prominent due higher residence time of the participating gases near the high temperature region. For higher values of strain rate, the flame becomes more stretched and chemical kinetics has a higher importance in the maintenance of the flame. Added to this, there is a higher formation of CO has residence time is lower, therefore, there is less complete combustion of the species, and the temperature reduces. In calculations considering adiabatic flames, the temperature would increase with the diminishing strain rate, as the scenario would be closer to an equilibrium. Figure 5.a presents the results for the radiative heat flux while Figure 5.b shows the curves of radiative heat source.

Table (2). Maximum values of molar fraction and temperature for different strain rates.

	5 s^{-1}	10 s^{-1}	20 s^{-1}	50 s^{-1}	100 s^{-1}
Temperature	1980 K	2026 K	2043 K	2039 K	2020 K
H_2O	0.1878	0.1868	0.1855	0.1835	0.1815
CO_2	0.0781	0.0748	0.0719	0.0680	0.0649
CO	3.43e-2	3.99e-2	4.26e-2	4.39e-2	4.42e-2

Figure 5.a presents the results for the radiative heat flux while Figure 5.b shows the curves of radiative heat source. As expected, with lower values of the velocity gradient, the radiative heat flux becomes higher, and therefore, accounts for radiative losses. In extreme cases, i.e., lower values of strain rate, these radiative losses could provoke the flame extinction, although this limit was not reached in the present calculations.

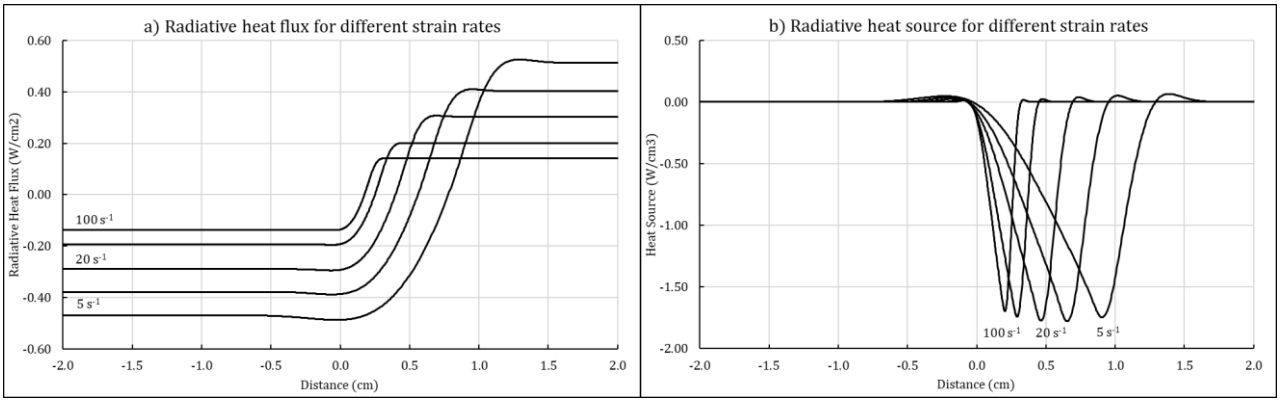

Figure 5. (a) radiative heat flux over distance and for different strain rates; (b) radiative heat source over distance and for different strain rates.

Sharing a similarity to what was perceived with temperature, the radiative heat source does not have a linear response to the strain rate. The minimum value for this quantity was calculated for the strain rate of 10 s^{-1}, decreasing in absolute value in both directions. Since a study of peak maximum temperature and minimum heat source over varying strain rates was not the focus of this work, it is unclear if both share the same value of strain rate as peak.

4.2 Models compared to the benchmark solution

The next step of this study was to compare the different formulations of the WSGG model with the LBL method. It should be noted that all formulations of the WSGG applied were developed for a fixed molar ratio, which it was not the case studied. Also, only Dorigon et al., 2013 and Coelho et al., 2019 originally validated their coefficients based on this same database used for calculation of the benchmark.

Figure 6a compares results for radiative heat flux for a strain rate of 10 s^{-1} while Figure 6b compares for the radiative heat source. For radiative heat source, the model with closest approximation to the LBL benchmark is the one proposed by Smith et al., 1982. On an interesting note, the work proposed by Dorigon et al., 2013, had achieved relative errors of maximum 5% and average 3%. However, in the scenario of a coupled solution of the radiation with the other equations that describe the flame, there is a significant increase in the error.

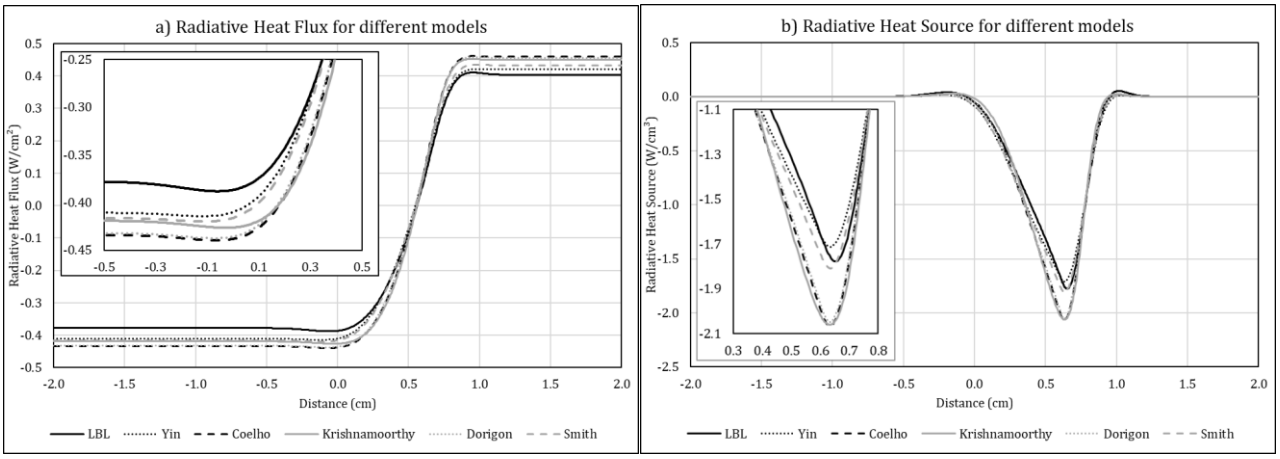

Figure 6. (a) radiative heat flux over distance and for different models; (b) radiative heat source over distance and for different models.

Since radiative losses impact on the overall temperature, that in its turn affect the formation and absorption of species, it is expected that differences between models become more accentuated as they are not anymore calculating the RTE for the same quantities of water vapor and carbon dioxide. Table 3 presents results of maximum and average error normalized by the maximum value of the WSGG models compared to the LBL solution for radiative heat flux and heat source. To understand this difference, is important to account for the fact that the model is proposed for a H_2O-CO_2 molar ratio of 2 to 1. However, in a counterflow flame, the molar ratio only achieves this ratio in the side of oxidant, as there is more incomplete combustion closer to the combustible.

Table 3. Maximum and average errors of WSGG models.

Model	Max q_R''	Avg q_R''	Max $\dot{q}_R$	Avg $\dot{q}_R$
Dorigon	13.2%	11.1%	17.1%	3.2%
Smith	9.2%	6.5%	6.7%	2.0%
Krishnamoorthy	13.3%	10.0%	20.9%	3.7%
Coelho	13.6%	11.8%	18.4%	3.1%
Yin	7.9%	4.6%	6.0%	2.0%

Figure 7 presents the error normalized by the maximum and the molar ratio as functions of distance for the formulation of the WSGG model proposed by Dorigon et al., 2013. The work proposed by this author is taken into consideration since it also assessed the results obtained with the LBL method.

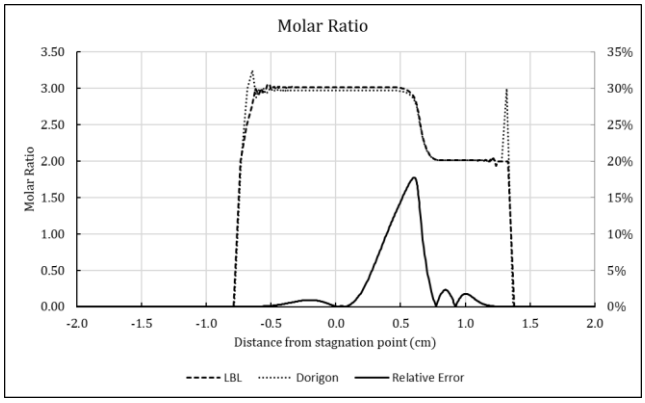

Figure 7. Error normalized by maximum and molar ratio.

As mentioned earlier, the radiative transfer equation solving is not a local evaluation of radiative properties, but an integrated process that obeys conservation of the radiative energy balance. Therefore, extrapolation of molar ratio may not impose a high relative error locally, but rather globally. Also, as part of the uniform initial formulation of the WSGG, the model may not be consistent when dealing with abrupt changes in the molar ratio, as seen in the region from 0.5 to 0.7 cm.

4.3 WSGG results for different strain rates

All models were calculated for the different values of strain rate and their results compared with the benchmark solution. Figure 8a presents results of the minimum (maximum in absolute value) of radiative heat source over strain rate for the different models and the benchmark as well, while Figure 8b presents this result for the maximum radiative heat flux. The benchmark result shows that there is a peak of minimum radiative heat source around the strain rate of 10 $^{s-1}$ and after it, as increasing the velocity gradient, the radiative heat source becomes lower in absolute value. However, one should keep in mind that not only the radiative heat source slightly decreases, but also the momentum of the flow is significantly higher in comparison, since the strain rate has increased over 10 times, which leaves the radiative losses more irrelevant in the scenario of higher strain rates. Interestingly, although the models proposed by Smith et al., 1982, and Yin, 2013, have closer results to the benchmark, neither model accompany the behavior of the curve of radiative heat source of the benchmark result, showing an increase of the radiative heat source as the strain rate also increases. On the other hand, the radiative heat flux can be well predicted by any of the models evaluated.

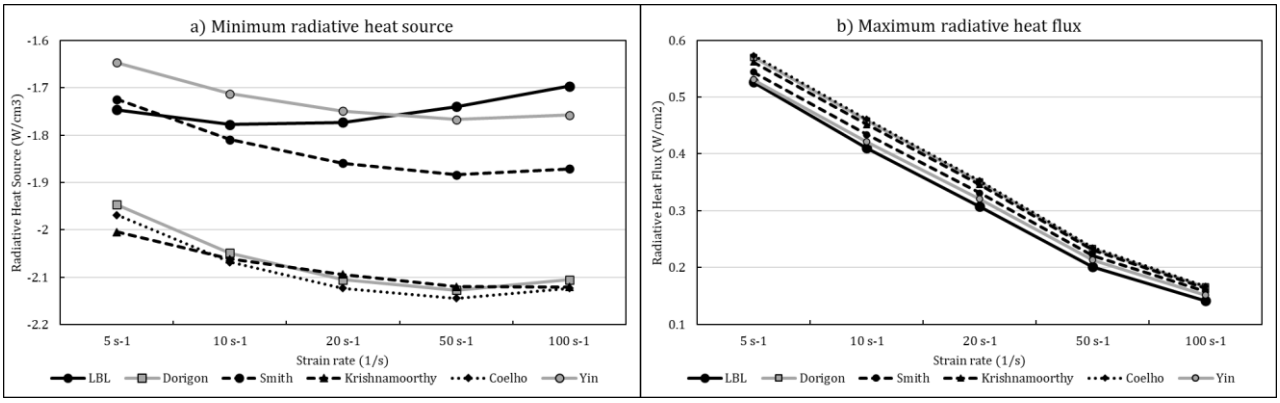

Figure 8. (a) radiative heat source over strain rate; (b) radiative heat flux over strain rate.

5. CONCLUSIONS

This paper presented an analysis of the accuracy of different formulations of the WSGG model based on coupled calculations carried out for laminar, counterflow flames. All comparisons were relative to the benchmark solution produced by the LBL integration of high-resolution absorption spectra provided by the HITEMP2010.

Results showed that the local error of the model in the prediction of the radiative quantities can be as high as 20%, although most models can adequately capture the behavior of the radiative quantities as the strain rate changes.

6. ACKNOWLEDGEMENTS

Author GCF thanks the National Council for Scientific and Technological Development (CNPq) for a postdoctoral scholarship. FHRF thanks CNPq for research grant 302686/2017-7.

7. REFERENCES

Coelho, F. and França, F.H.R., 2019. “WSGG correlations based on HITEMP2010 for gas mixtures of H_2O and CO_2 in high total pressure conditions”. *International Journal of Heat and Mass Transfer*, Vol. 127, pp. 105-114

de Goey, L.P.H. and Boonkkamp, J.H.M.T., 1999. “A flamelet description of premixed laminar flames and the relation with flame stretch”. *Combustion and Flame*, Vol. 119, pp. 253-271.

Dorigon, L.J., Duciaki, G., Brittes, R., Cassol, F., Galarça, M. and França., F.H.R., 2013. “WSGG correlations based on HITEMP2010 for computation of thermal radiation in non-isothermal, non-homogeneous H_2O/CO_2 mixtures”. *International Journal of Heat and Mass Transfer*, Vol. 64, pp. 863–873.

Fraga, G.C., Zannoni, L., Centeno, F.R. and França, F.H.R., 2019. “Evaluation of different gray gas formulations against line-by-line calculations in two- and three-dimensional configurations for participating media composed by CO_2, H_2O and soot”. *Fire Safety Journal*, Vol. 108.

Fraga, G.C., Bordbar, H., Hostikka, S. and França, F.H.R., 2020. “Benchmark Solutions of Three-Dimensional Radiative Transfer in Nongray Media Using Line-by-Line Integration”. *Journal of Heat Transfer*, Vol. 142.

Goswami, M., 2014. *Laminar burning velocities at elevated pressures using the heat flux method*. Eindhoven University of Technology. https://doi.org/10.6100/IR766389

Howell, J.R., Menguç, M.P. and Siegel, R., 2016. *Thermal Radiation Heat Transfer*. Taylor & Francis Group, Florida, USA.

Kazakov, A. and Frenklach, M., 1995. *Reduced Reaction Sets based on GRI-Mech 1.2*. University of California at Berkeley. http://www.me.berkeley.edu/drm/

Krishnamoorthy, G., 2010. "A new weighted-sum-of-gray-gases model for CO_2-H_2O gas mixtures". *International Communications in Heat and Mass Transfer*, Vol 104, pp. 602-608.

Rothman, L.S., Gordon, I.E., Barber, R.J., Dothe, H., Gamache, R.R., Goldman., A., Perevalov, V., Tashkun, S.A., Tennyson, J. 2010. "HITEMP, the high-temperature molecular spectroscopic database". *Journal of Quantitative Spectroscopy and Radiative Transfer*, Vol. 111, pp. 2139–2150.

Smith, T.F., Shen, Z.F. and Friedman, J.N., 1982. "Evaluation of Coefficients for the Weighted Sum of Gray Gases Model". *Journal of Heat Transfer*, Vol 37, pp. 1182-1186.

Somers, B., 1994. *The simulation of flat flames with detailed and reduced chemical models.* Eindhoven University of Technology.

Yin, C., 2013. "Refined Weighted Sum of Gray Gases Model for Air-Fuel Combustion and Its Impacts". *Energy and Fuels*, Vol. 27, pp.-507-514.

8. RESPONSIBILITY NOTICE

The authors are the solely responsible for the printed material included in this paper.